Journal of Machine Engineering, 2022, Vol. 22
ISSN 1895-7595 (Print) ISSN 2391-8071 (Online)

Received: *10 May. 2022* / Accepted: *18 June 2022* / Published online: *28 June 2022*

steam turbine, blade throat,
3D optical scanning,
geometric deviation

Petr ERET[1*], Michal HOZNEDL[2]

ANALYSIS OF GEOMETRIC ERRORS OF THROAT SIZES OF LAST STAGE BLADES IN A MID-SIZE STEAM TURBINE

Steam turbine technology with enhanced flexibility will continue to participate in electric power supply mixes. Last stage blades secure the reliability of a steam turbine and require high precision manufacturing and assembly. This case study presents a statistical analysis of geometric errors of the throat sizes of the last stage blades in a mid-size steam turbine. A 3D optical scanner is employed to capture detailed geometries of rotor blades and a half of assembled nozzle diaphragm. Unrolled cylinder cross-sections are used to evaluate 2D geometrical features such as blade throats and areas at three different diameters, and the results are compared to intended designs. In addition, linear correlations between the throat size and blade pitch, area and trailing edge thickness are established, and blade throat position shifts are quantified. Such a comprehensive study is presented for the first time, and some useful conclusions can be retrieved from this case study.

1. INTRODUCTION

There will be a need for more electricity across various geographies, and global electricity consumption more than doubles over the next 40 years [1]. Despite the increasing importance of renewable energy [2], steam turbine technology with improved flexibility will contribute to electric power supply mixes [3, 4]. Baseload thermal power plants must operate under variable loads due to wind and solar energy share. Steam turbines are subject to severe operating conditions [5, 6], and rotor last stage blades can operate in a compressor mode delivering energy to the working fluid in low volume flow conditions [7]. Concepts of a dynamic power plant and solutions for an operational flexibility enhancement appear more often in the literature [8–12].

Many components of steam turbines require high precision manufacturing processes to ensure a long and safe operating life, also in off-design conditions [13]. In particular, last stage blades are the essential component securing the reliability of a steam turbine for thermal and nuclear power plants. Recently machining processes of the long blades have become fully automated by using five-axis milling machines [14]. However, due to complicated tool path

[1] Dept. of Power System Engineering, Faculty of Mechanical Engineering, University of West Bohemia, Czech Republic
[2] Experimental Research of Flow, Doosan Skoda Power, Czech Republic
[*] E-mail: petreret@kke.zcu.cz
https://doi.org/10.36897/jme/151118

planning, limited machining precision or unexpected machining errors, deviation of blades from the nominal design is unavoidable [15–17]. Turbine blade profiles often become thinner or thicker than the nominal profiles because of the manufacturing tolerances, which directly determine the costs of the manufacturing of turbine blades. The reduction of tolerances requiring greater engineering complexity and accuracy leads to increased production costs, and the investigation of manufacturing errors in turbomachinery already started several decades ago [18]. For instance, Bammert and Sandstede [19] have reported that variation of aerodynamic performance was almost linearly dependent on the manufacturing tolerance. In addition to manufacturing errors, turbine blade disk assembly must be of good quality to guarantee trouble-free operation and required performance [20]. Geometric deviations of blades caused by manufacturing or assembly errors are typically minor compared to blade sizes. However, they have identifiable performance impacts, as shown by many authors [21–27]. Salehi et al. [28] pointed out that it is generally difficult to characterise geometrical uncertainties in terms of probabilistic distribution functions, and in many engineering calculations, the geometrical uncertainty inputs are usually modelled using a normal distribution.

In steam turbine blade design, there are several geometric parameters with effects on aerodynamic performance. For example, Zhang et al. [29] have emphasised the importance of leading edge geometry on a 5-stage low-pressure turbine and Wang et al. [30] have studied the effect of the blade geometry near the trailing edge in a high-subsonic-turbine cascade. Sieverding and Manna [31] have reviewed thoroughly the turbine trailing edge flow and its impact on the blade performance. Ding et al. [32] investigated the entropy generation and exergy destruction of condensing steam flow in a turbine blade with roughness. The most critical geometric parameter of bladed disks is the throat area, which defines the turbine capacity (mass flow rate passing through the turbine stage). Chen et al. [20] have analysed assembly errors with the effect on throat and incidence for turbine blades. Two types of error (Circumferential Indexing Error and Axial Positioning Error) have been defined, and their influence on the power output and the efficiency of a turbine was explained. However, the authors showed only the distribution and variation of both errors for rotor blades and no direct quantification of the throat size had been demonstrated. It was reported that such assembly errors could also result in the non-uniform distribution of shape, mass and stiffness of bladed disks, and this may cause dynamic unbalance, mistuning and vibration in the operational process of turbomachinery.

A statistical analysis of geometric errors of the throat sizes of the last stage blades in a mid-size steam turbine is performed in this work. A 3D optical scanner is employed to obtain detailed measurement information of half of the assembled nozzle diaphragm and all rotor blades. Unrolled cylinder cross-sections are constructed to evaluate geometric features such as blade throat and area at three diameters. Histograms are created based on the obtained values, and discrepancies between nominal and mean values are found. In addition, linear correlations between the throat size and blade pitch, area and trailing edge thickness are established. The work is completed by an investigation of the blade throat position shift. Such a comprehensive study is presented for the first time, and while the results are mainly conditioned by the given manufacturing processes, some useful conclusions can be retrieved from this case study.

2. INVESTIGATED GEOMETRIES AND ANALYSIS TOOLS

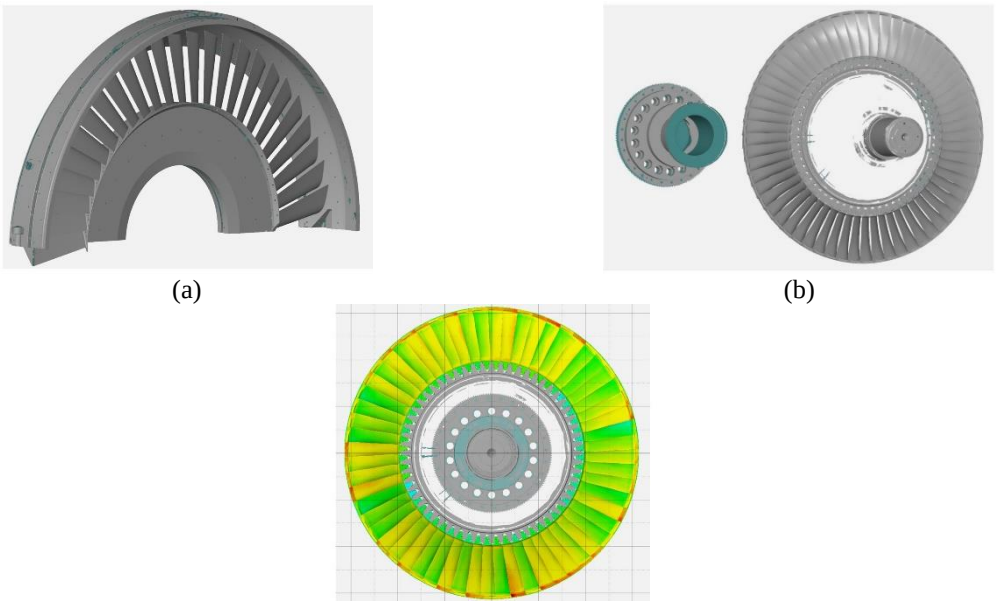

(a) (b)

(c)

Fig. 1. Actual geometry: (a) upper half of nozzle diaphragm, (b) rotor last stage blades, (c) surface deviation map of rotor blades - upstream view

The examined objects are the last stage blades of a synchronous steam turbine with a rated rotational speed of 3000 RPM and a mid-size power output before it is put into use. Figure 1a shows the actual geometry of the upper half of the diaphragm. The diaphragm consists of 25 nozzle blades inserted into the outer and inner rings, which are mechanically secured by pins to minimise deformation and improve manufacturing accuracy. It should be emphasised that the diaphragm is assembled and not welded as typical for diaphragm fabrication. The hub radius is about 790 mm, and the total length of the stator blade is 420 mm at the trailing edge. The lower part of the diaphragm is not detailed, as similar conclusions were drawn for both parts. Figure 1b also depicts the actual geometry of the rotor with 60 last stage blades. Each blade of a total length of 460 mm has a fir-tree root and an integral tip shroud. Unfortunately, more details on the basic geometrical characteristics of the turbine blades are not available to the public.

Modern optical scanners can construct exact 3D digital models [33, 34]. A GOM ATOS III Triple Scan + TRITOP digitising system, which is an industry-standard system used by many leading manufacturing companies, is employed in the current study. The system uses advanced projection technology of structured blue light and features two 8 megapixel cameras that can provide a typical point spacing of 0.01 mm. The device is characterised by high performance, fine detail resolution and highly accurate datasets. All measurements are automatically transformed into a common object coordinate system. The system oversees both calibration and influence of environmental conditions, and efficient measurements can be made under laboratory or industrial conditions. The complete 3D dataset is exported using standard file formats for post-processing. GOM Inspect software performed actual mesh/model global best-fit alignments and constructions of unrolled cylinder cross-sections.

Figure 1c shows the example of a surface deviation map between the actual and model geometry of the rotor. The map is displayed in the RGB colour model, where red is the maximum discrepancy, green represents the zero deviation, and blue is the minimum discrepancy; however, the colour range is confidential. Unrolled cylinder cross-sections are constructed at three diameters – near blade root, mid-span and blade tip, as shown in Fig. 2. An example of unrolled cylinder cross-section of rotor blades with areas and throats at the blade tip diameter is depicted in Fig. 3. A blade throat is determined using a minimal distance search algorithm between two curves. Datasets were further processed in Matlab to evaluate the geometric variability of blade throat and area, and histograms were used to display the estimates. Data are normalised to nominal values, and relative deviations are given as a percentage with nominal values set to zero. The optimal numbers of bins in histograms have been calculated using a technique proposed by Shimazaki and Shinomoto [35].

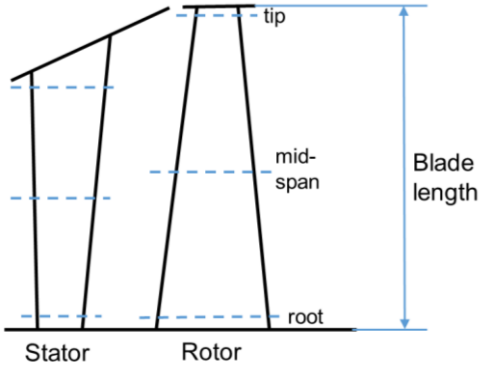

Fig. 2. A schematic of turbine blade stage with three diameters for unrolled cylinder cross-sections

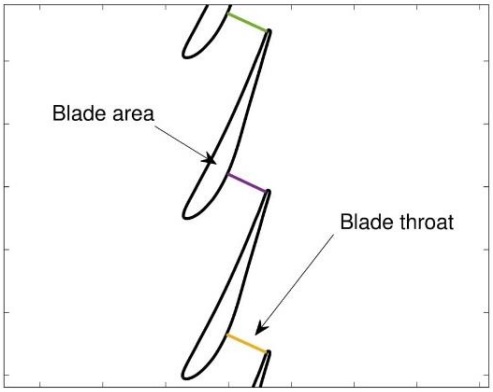

Fig. 3. Unrolled cylinder cross-section of rotor blades with areas and throats at the blade tip diameter

The relation between the blade throat size and blade area, pitch and trailing edge thickness for the rotor blades is also investigated. Blade pitches are estimated by the differences in the centre of gravity of adjacent blades rather than using a trailing edge spacing, as the geometry of the thin trailing edge is susceptible to huge manufacturing and assembly errors. The issue is demonstrated by estimating the diaphragm blade mid-span pitch in Fig. 4,

which compares histograms between the two mentioned approaches. While the mean values are nearly identical, the error range of blade pitch estimation based on the trailing edge spacing is over two times larger than in the blade centre of gravity approach. The nominal trailing edge thickness is around 1.2 mm in this particular case. Considering a typical positive manufacturing tolerance of 0.1 mm, the error between the nominal and tolerated trailing edge thickness is implicitly large, nearly 17%. Since trailing edges are finished by hand manufacturing, a trailing edge thickness is estimated in a blade throat plane instead of a circle fitting of the trailing edge, which proved inaccurate and unsuitable for further analysis. The estimation is illustrated in Fig. 5, where the blade throat line intersects the lower and the upper curve of the blade profile and the distance between the intersection points represents the trailing edge thickness.

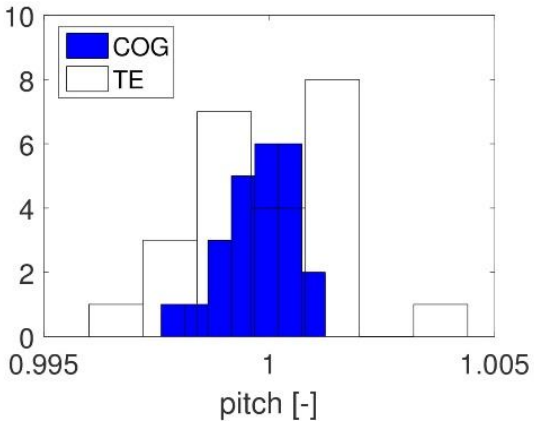

Fig. 4. A comparison between two histograms for diaphragm blade pitch based on blade centre of gravity (COG) and trailing edge (TE)

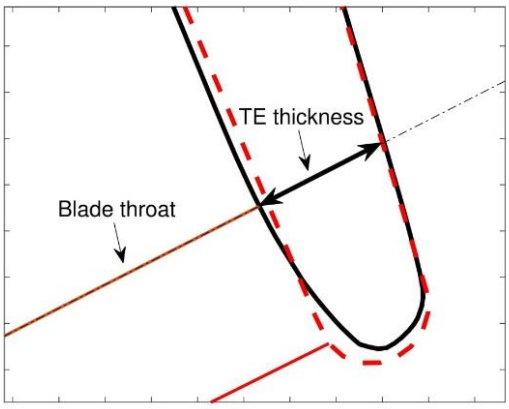

Fig. 5. Trailing edge of stator blade in mid-span: actual (-) and nominal (- - -)

The analysis is completed by evaluating the Pearson correlation coefficient *R*, which quantifies the strength of a linear relationship between two variables. It has a value between +1 (total positive linear correlation) and –1 (total negative linear correlation) and is zero for no linear correlation. The parameter is defined in Eq. 1,

$$R = \frac{\sum_{i=1}^{n}(x_i - \bar{x})(y_i - \bar{y})}{\sqrt{\sum_{i=1}^{n}(x_i - \bar{x})^2 \sum_{i=1}^{n}(y_i - \bar{y})^2}} \tag{1}$$

where n is the sample size, x_i and y_i are the individual sample points indexed with i and $\bar{x}$ represents the sample mean (analogously for $\bar{y}$). There might be a tendency for the values of the variables to increase or decrease in tandem. The relationship between two variables is generally considered strong when the absolute value of $|R|$ is larger than 0.7, moderate for $0.7 > |R| > 0.5$, weak for $0.5 > |R| > 0.3$ and none or very weak for $|R| < 0.3$.

3. RESULTS

3.1. DIAPHRAGM BLADES

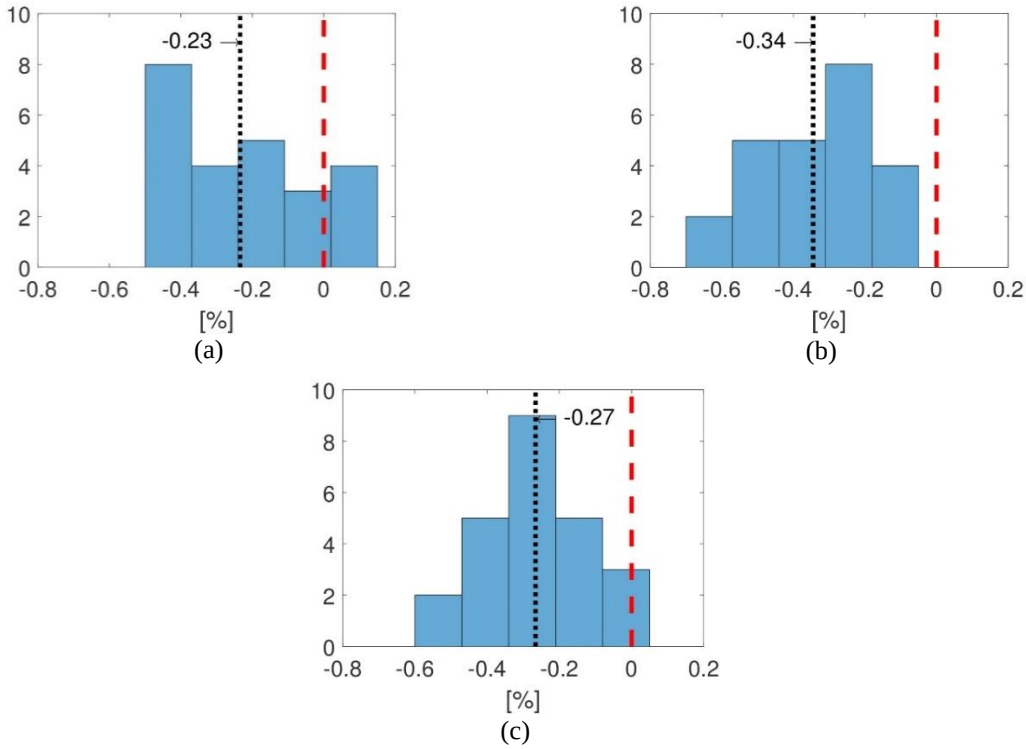

Fig. 6. Histograms of diaphragm blade throat: (a) root, (b) mid-span, (c) tip; mean (⋯) and nominal (- - -)

Figure 6 shows the distribution of diaphragm blade throat estimates at three different diameters. The histogram pattern at the blade root is multimodal, the histogram at the blade mid-span is slightly skewed left, and the histogram pattern at the tip diameter is symmetric and unimodal. The vast majority of the blade throats are smaller than the nominal values. The error between the nominal and mean values is –0.23% at the blade root, –0.34% at the blade mid-span, and –0.27% at the blade tip.

Figure 7 depicts the histograms of blade area at three different diameters. The histogram at the blade root is slightly skewed left, the histogram at the blade mid-span is slightly skewed right, and the histogram pattern at the tip diameter is skewed right. The actual blade areas are slightly bigger than the design intents at all diameters, with mean errors of around 1%. Positions of histograms to the nominal values suggest that the manufacturing of diaphragm blades is precise but a bit inaccurate.

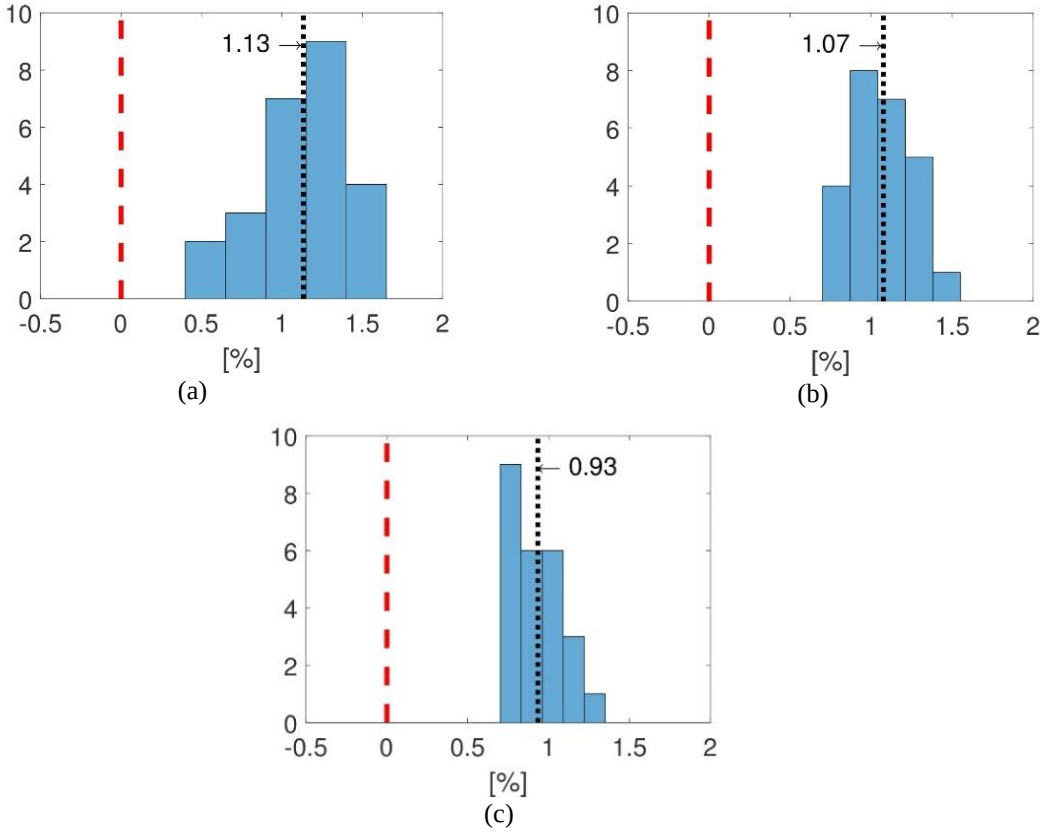

Fig. 7. Histograms of diaphragm blade area: (a) root, (b) mid-span, (c) tip; mean (⋯) and nominal (- - -)

Figure 8 shows the relations between the blade throat size and blade area, pitch and trailing edge thickness at the blade root. For clarity, the scatter plots are supplemented by linear regressions. The analysis revealed a strong relationship with a negative correlation coefficient $R = -0.72$ between the blade throat and the trailing edge thickness at the blade root; the blade throat decreases with the increasing trailing blade thickness. However, this relation becomes weak at the blade tip and the mid-span, as shown in Table 1, which summarises the blade throat correlation coefficients R for diaphragm blades. It is important to note that the error between the actual and nominal trailing edge thickness can be huge, up to 35% (see the bottom of Fig. 8) and differs at least by one order of magnitude from the errors in blade throat, pitch or area. Consistency can be found in the blade throat/pitch relation for all blade diameters. This correlation is positive with moderate strength as the blade throat increases with the increasing blade pitch, and the relationship is more robust with

the increasing diameter. Finally, the analysis has confirmed the opposite relation between the blade throat and the blade area (see Figs. 6 and 7). This relationship has a negative correlation coefficient with moderate to weak strength depending on the blade diameter, as detailed in Table 1).

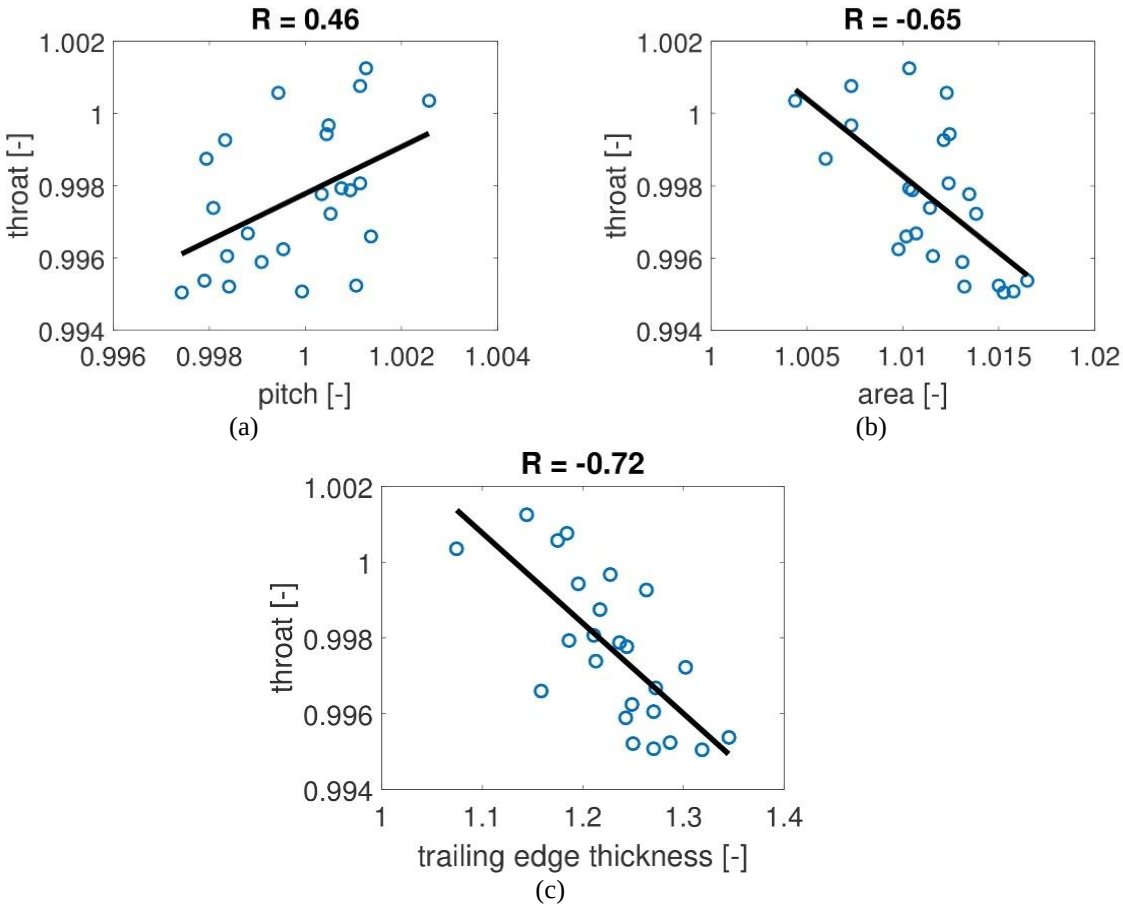

Fig. 8. Diaphragm blade throat correlations at the root diameter: (a) pitch, (b) area, (c) trailing edge thickness

Table 1. Blade throat correlation coefficient *R*, diaphragm blades

Blade diameter	Pitch	Area	TE thickness
root	0.46	-0.65	-0.72
mid-span	0.53	-0.53	-0.24
tip	0.60	-0.38	-0.36

3.2. ROTOR BLADES

Figure 9 shows the histograms of rotor blade throat estimates at three different diameters. In comparison to the nominal values, blade throats are smaller again, but the percentage differences between the nominal and mean values are far larger than in the diaphragm blades. In particular, the discrepancy at the blade root is –1.61%, which is seven

times larger than the corresponding value of –0.23% quantified for the stator blades. A similar value of the deviation of –1.59% has been found at the blade tip, which is nearly six times greater than the analysis of diaphragm blades (–0.27%). Finally, the difference of –1.16% between the nominal and mean value has emerged at the mid-span of the rotor blade, and this is almost three and half times larger than the corresponding value of -0.34% evaluated for the stator blades. The histogram patterns in Fig. 9 are unimodal, and only the histogram at the blade tip is symmetric. Figure 10 depicts the data distribution for rotor blade area at three different diameters, and the histograms are again approximately unimodal. All manufactured blades are substantially larger than the nominal profiles. The percentage differences between the nominal and mean values are about 4% at both blade root and mid-span diameters, and the discrepancy at the blade tip is 8.43%. Thus, the manufacturing of rotor blades can be considered precise but not accurate

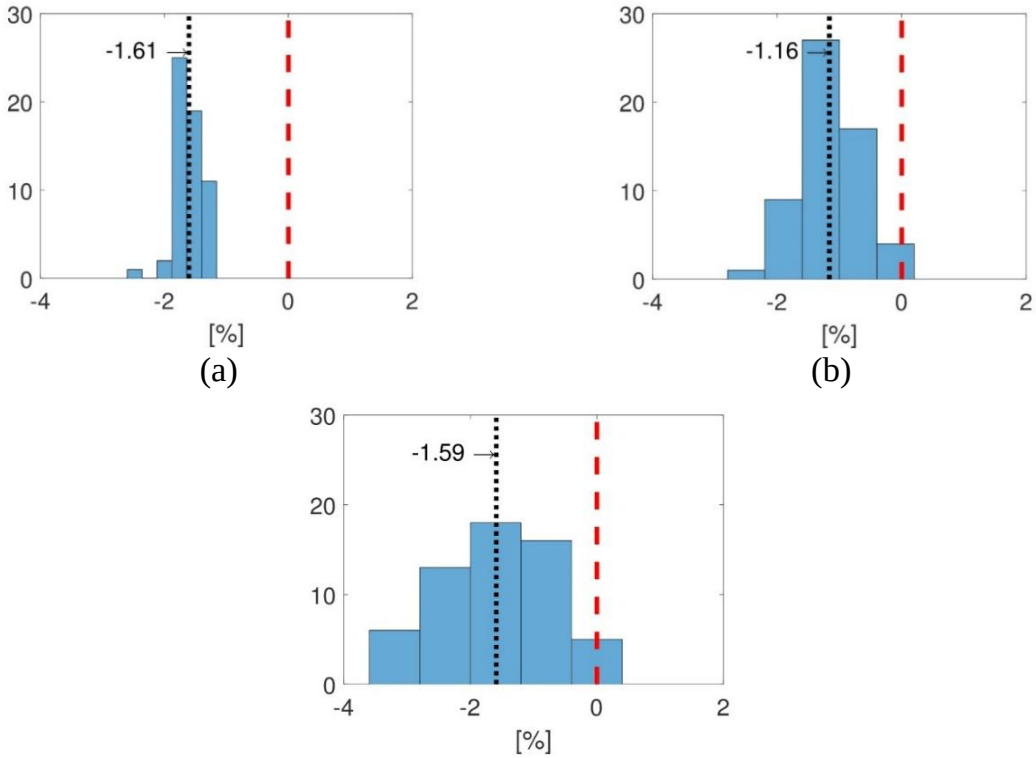

Fig. 9. Histograms of rotor blade throat: (a) root, (b) mid-span, (c) tip; mean (⋯) and nominal (- - -)

Figure 11 shows the scatter plots with linear regressions between the rotor blade throat and the blade pitch at three different diameters. A very weak linear relationship has been detected at the blade root. Positive associations between the variables have been found at blade mid-span and tip diameters, and the relationship is stronger as the diameter increases. A high correlation coefficient $R = 0.88$ can be observed at the blade tip as the datasets group closer together in a linear shape. The finding means that the blade throat size is highly susceptible to blade pitch alignment.

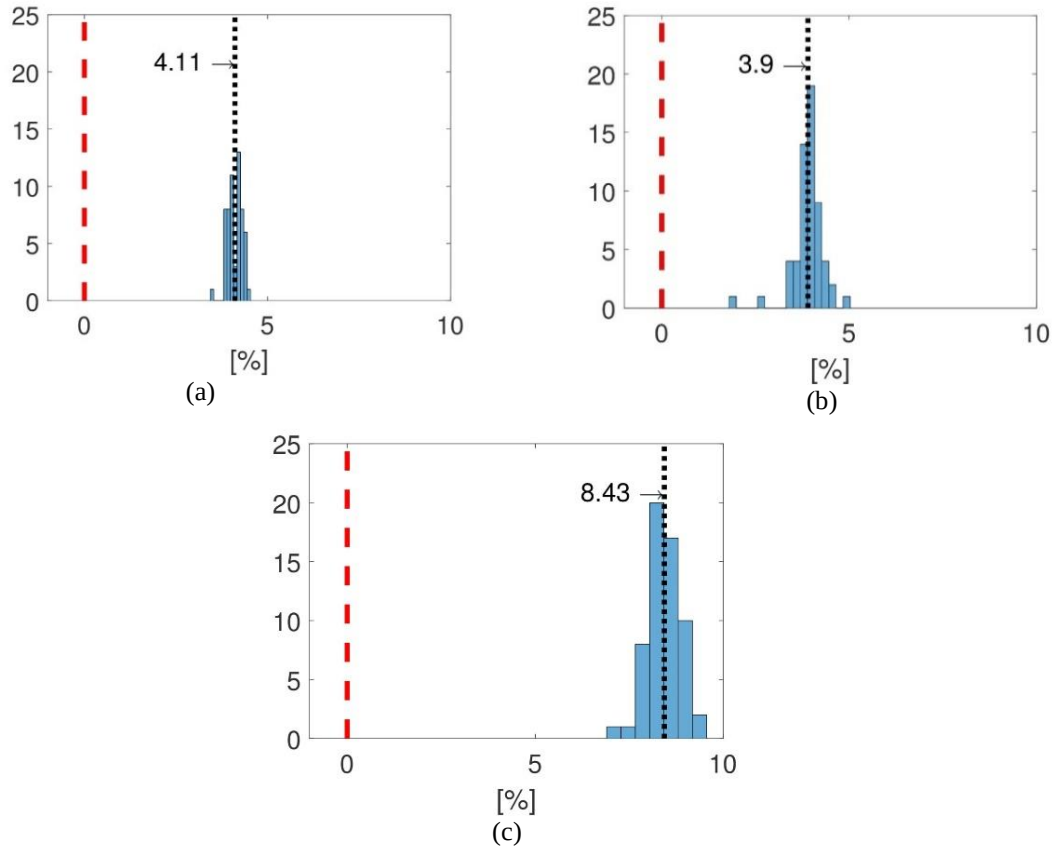

Fig. 10. Histograms of rotor blade area: (a) root, (b) mid-span, (c) tip; mean (⋯) and nominal (- - -)

Table 2 summarises the blade throat correlation coefficients *R* for the rotor blades. Negative relations with none or very weak strength have been identified between the rotor blade throat and both blade area and trailing edge thickness at all diameters. The trends observed in Table 1 and Table 2 are reasonably coherent for the correlation between the throat size and the blade pitch. Both stator and rotor blade throat sizes are more prone to blade pitch alignment as the diameter increases. Consistency for all blades at larger diameters can be found in the blade throat size/area relation. The blade throat size increases with the decreasing blade area, and this relation is weaker at a larger diameter. Excluding the result for stator blades at the blade root, the overall findings have shown that the trailing edge thickness has a minimum impact on the blade throat size as the correlation coefficients are small. However, the values of the correlation coefficients are generally case-dependent. For this study case, it can be concluded that only pitch alignment of rotor blades has a substantial impact on the blade throat size for larger diameters and other geometrical parameters are of minor importance.

Figure 12 shows the rotor blade throat and trailing edge thickness relation at the blade tip. It can be emphasised that the errors between the actual and nominal trailing edge thickness can be over 50% and are notably larger than the errors in blade throats, pitches or areas. This outcome is correct as the trailing edge thickness represents a small geometric dimension sensitive to manufacturing errors.

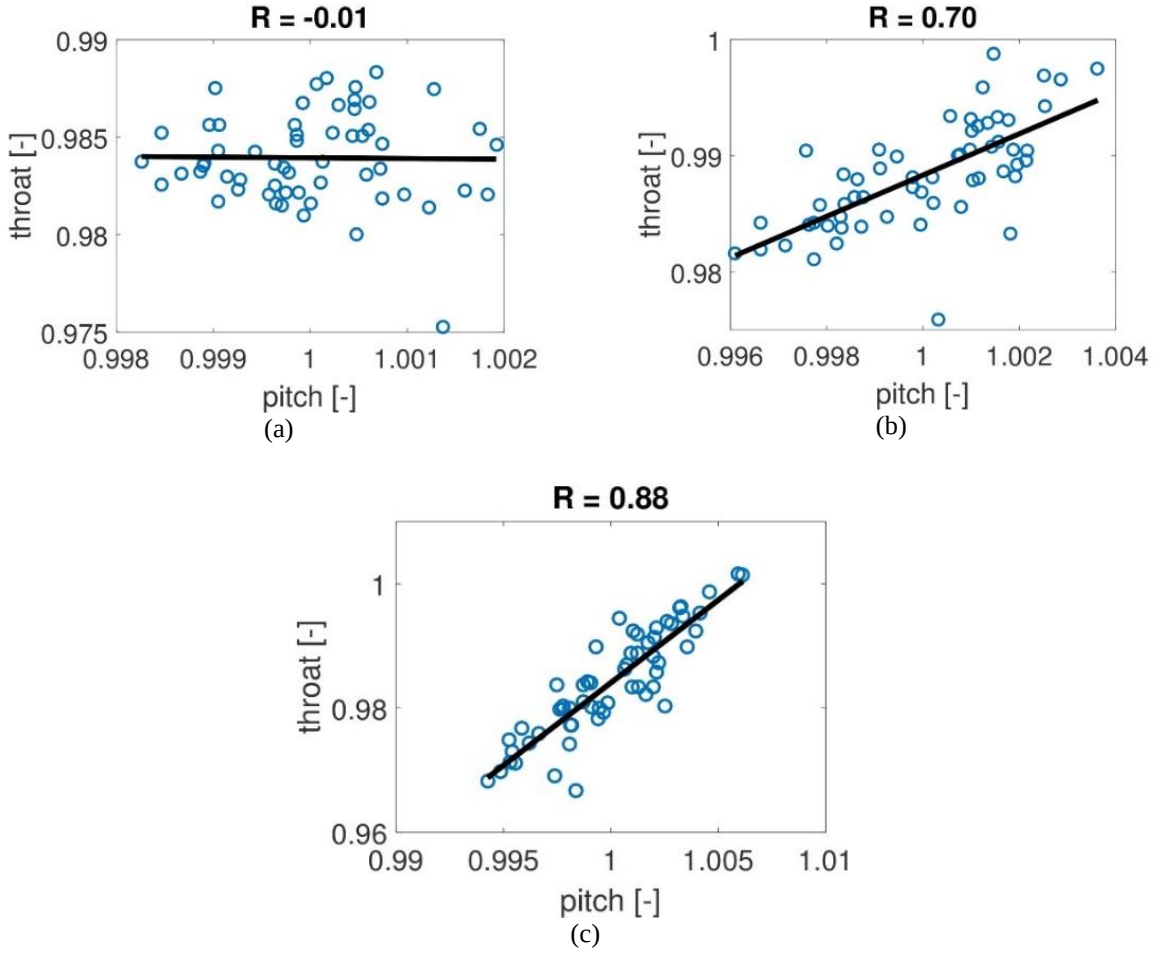

Fig. 11. Correlation between rotor blade pitch and throat: (a) root, (b) mid-span, (c) tip

Table 2. Blade throat correlation coefficient *R*, rotor blades

Blade diameter	Pitch	Area	TE thickness
root	–0.01	–0.27	0.02
mid-span	0.70	–0.32	–0.17
tip	0.88	–0.07	–0.29

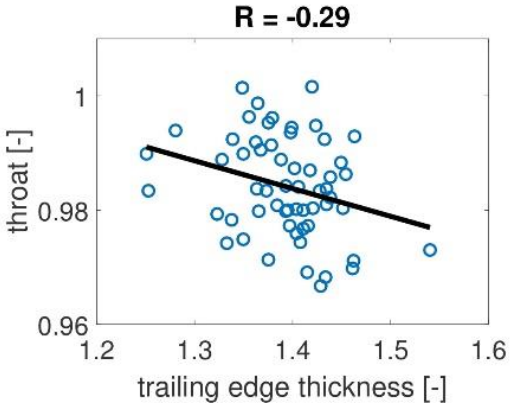

Fig. 12. Rotor blade throat and trailing edge thickness relation at blade tip

3.3. BLADE THROAT POSITION SHIFT

The actual blade throat position is equally important to the blade throat size. The incorrect location of the throat in the blade channel can affect the distribution of Mach number and pressure. No considerable deviations in the position of actual blade throats to the nominal blade throat have been found for both stator and rotor geometries. Fig. 13 shows the actual and nominal blade throat position at the rotor blade tip. The vector plot in Fig. 14 depicts the shifts of centre position (related to the nominal blade throat size – th_{nom}) between the actual and nominal blade throat for all rotor blade tips. The maximum value of 1.66 mm (4.7% of th_{nom}) has been detected, and the vast majority of actual blade throats are located upstream of the nominal blade throat. Given the blade dimensions, the minor blade throat dislocations will cause no effect on the actual fluid flow.

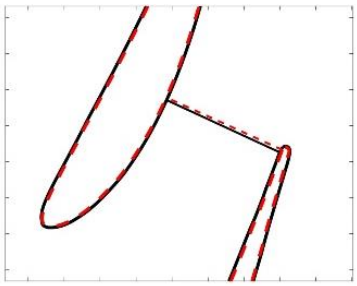

Fig. 13. Actual and nominal blade throat position at the rotor blade tip: actual (-) and nominal (- - -)

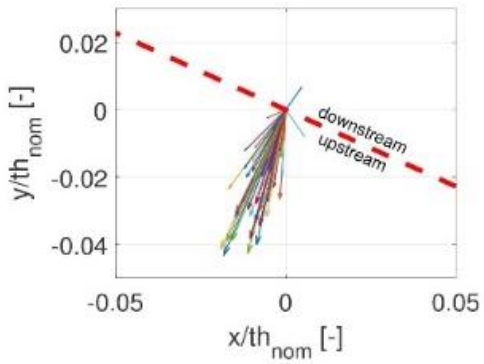

Fig. 14. Relative shifts of blade throat centre at the blade tip: position of nominal throat – centre section (- - -)

4. DISCUSSION

Manufactured blades are often thinner or thicker than nominal profiles. Thinning of blade profiles can lead to a mass flow increase and a decrease of the enthalpy drop of the turbine, while the opposite effect can be observed for thicker blades. Both thinning and thickening of blade profiles decrease the efficiency and the lifetime of turbines; however, thicker blades can perform significantly worse [18]. In the context of the current investigation, there is an opportunity to improve the last stage performance through advanced precision manufacturing.

On the other hand, steam turbine blades at low-pressure stages may be eroded by wet steam flow, which causes thinning of blade profiles. Erosion reduces the efficiency of the last stage rotor blades and makes the operational lifetime of the turbine shorter [36]. Even erosion-resistant materials for steam turbine blades, such as laser-hardened steels or titanium alloys, are prone to loss of material [37], and therefore, manufacturing thicker blade profiles can be justifiable. However, any considerations to support the existing technology or advanced precision manufacturing are beyond the scope of this study.

The good agreement of the investigated diaphragm with the nominal geometry is caused by the manufacturing method applied here, i.e. assembling the individually machined parts without any welding. Welding is the most common technique of diaphragm fabrication, and large deformations and residual stresses are produced. It can be plausibly anticipated that the discrepancy between welded and nominal blades will be dramatically different, and hence similar investigations will be more than worthwhile.

5. CONCLUSION

A statistical analysis of geometric errors of the throat sizes of the last stage blades in a mid-size steam turbine has been performed on the actual geometry and compared to the design model. A 3D optical scanner was used to obtain the actual meshes of the upper part of assembled nozzle diaphragm and rotor blades. Blade throats and areas at three different diameters were evaluated in unrolled cylinder cross-sections.

It was found that the diaphragm blade throats are smaller than the intended design, and the most significant deviation between the nominal and mean values was –0.34%. The rotor blade throats were also smaller than initially supposed, but the percentage differences between the nominal and mean values were far larger than in the case of diaphragm blades. The minimal difference of –1.16% between the nominal and mean value has been evaluated at the rotor blade mid-span, almost three and half times larger than the corresponding value of –0.34% related to the stator blades. In terms of blade area, the diaphragm blades are slightly bigger than the design intent, with mean errors of around 1%. On the other hand, the manufactured rotor blades were substantially larger than the nominal profiles.

The percentage differences between the nominal blade area and the mean values were about 4% at both blade root and mid-span diameters, and the discrepancy at the blade tip was 8.43%. Therefore, it was concluded that the manufacturing of both stator and rotor blades is precise, but the accuracy of the blade machining can be improved, especially in the case of rotor blades.

Linear correlations between the throat size and blade pitch, area and trailing edge thickness have been established. In the case of diaphragm blades, the analysis revealed a strong relationship with a negative correlation coefficient $R = -0.72$ between the blade throat and the trailing edge thickness at the diaphragm blade root. However, this relation became weak at the blade mid-span and the blade tip. Negative relation has also been found between the blade throat and the blade area, with moderate strength at the blade root and the mid-span and weak strength at the blade tip. The blade throat/pitch relation was positive with moderate strength for all diameters and grew stronger with the increasing diameter. In the rotor blades,

a high-value correlation coefficient $R = 0.88$ was observed at the blade tip for the rotor blade throat and the blade pitch relation. This positive relationship was also strong at the blade mid-span but none at the blade root. The finding suggests that the rotor blade throat size is susceptible to blade pitch alignment. Finally, negative relations with none or very weak strength have been identified between the rotor blade throat and both blade area and trailing edge thickness at all diameters. It can be concluded that only pitch alignment of rotor blades has a substantial impact on the blade throat size for larger diameters and other geometrical parameters are of minor importance.

This study was completed by investigating the blade throat position shift to the nominal geometry, and no considerable deviations of actual blade throat locations have been found for both stator and rotor geometries. The quality of production and assembly of blades is essential for the performance and safe operation of turbomachinery. Unfortunately, the investigation of geometric errors in blades receives little attention in the literature, and this case study presented a comprehensive statistical study of throat sizes in mid-size steam turbine last stage blades for the first time. The results provided a clear understanding of the precision and accuracy of the manufactured blades and gave direct feedback to improve the manufacturing and assembly of last stage blades.

ACKNOWLEDGEMENTS

This study was financially supported by the Ministry of Education, Youth and Sports of the Czech Republic under grant agreement No. CZ.02.1.01/0.0/0.0/16 026/0008389. The authors also thank Doosan Skoda Power for the permission to publish this paper and the 3D Scanning and Reverse Engineering Team of Doosan Skoda Power for providing the data.

REFERENCES

[1] KOBER T., SCHIFFER H.W., DENSING M., PANOS V., 2020, *Global Energy Perspectives to 2060 – WEC's World Energy Scenarios 2019*, Energy Strategy Reviews, 31, 100523.

[2] GIELEN D., BOSHELL F., SAYGIN D., BAZILIAN M.D., WAGNE N., GORINI R., 2019, *The Role of Renewable Energy in the Global Energy Transformation*, Energy Strategy Reviews, 24, 38–50.

[3] FUNAHASHI N., 2017, 22 – *Steam Turbine Roles and Necessary Technologies for Stabilization of the Electricity Grid in the Renewable Energy Era*, Advances in Steam Turbines for Modern Power Plants, Tanuma T., Ed., Woodhead Publishing, 521–537.

[4] TOPEL M., LAUMERT B., 2018, *Improving Concentrating Solar Power Plant Performance by Increasing Steam Turbine Flexibility at Start-Up*, Solar Energy, 165, 10–18.

[5] MEGERLE B., MCBEAN I., STEPHEN RICE T., OTT P., 2014, *Unsteady Aerodynamics of Low-Pressure Steam Turbines Operating Under Low Volume Flow*, Journal of Turbomachinery, 136, 091008.

[6] HONG H., WANG W., LIU Y., 2019, *High-Temperature Fatigue Behavior of a Steam Turbine Rotor Under Flexible Operating Conditions with Variable Loading Amplitudes*, International Journal of Mechanical Sciences, 163, 105121.

[7] BEEVERS A., HAVAKECHIAN S., MEGERLE B., 2015, *On the Prediction and Theory of the Temperature Increase of Low Pressure Last Stage Moving Blades During Low Volume Flow Conditions, and Limiting it Through Steam Extraction Method*, Journal of Turbomachinery, 137, 101002.

[8] ZHAO Y., WANG C., LIU M., CHONG D., YAN J., 2018, *Improving Operational Flexibility by Regulating Extraction Steam of High-Pressure Heaters on a 660 MW Supercritical Coal-Fired Power Plant: A Dynamic Simulation*, Applied Energy, 212, 1295–1309.

[9] RICHTER M., OELJEKLAUS G., GORNER K., 2019, *Improving the Load Flexibility of Coal-Fired Power Plants by the Integration of a Thermal Energy Storage*, Applied Energy, 236, 607–621.

[10] STEVANOVIC V.D., PETROVIC M.M., MILIVOJEVIC S., ILIC M., 2020, *Upgrade of the Thermal Power Plant Flexibility by the Steam Accumulator*, Energy Conversion and Management, 223, 113271.
[11] NOWAK G., RUSIN A., LUKOWICZ H., TOMALA M., 2020, *Improving the Power Unit Operation Flexibility by the Turbine Start-Up Optimization*, Energy, 198, 117303.
[12] RUSIN A., NOWAK G., LUKOWICZ H., KOSMAN W., CHMIELNIAK T., KACZOROWSKI M., 2021, *Selecting Optimal Conditions for the Turbine Warm and Hot Start-Up*, Energy, 214, 118836.
[13] EMONTS D., SANDERS M.P., MONTAVON B., SCHMITT R.H., 2022, *Model-Based, Experimental Thermoelastic Analysis of a Large Scale Turbine Housing*, Journal of Machine Engineering, 22/1, 84–95.
[14] MCBEAN I., 2017, *16 – Manufacturing Technologies for Key Steam Turbine Parts*, Advances in Steam Turbines for Modern Power Plants, Tanuma T., Ed., Woodhead Publishing, 381–393.
[15] ZHOU Y., CHEN Z.C., YANG X., 2015, *An Accurate, Efficient Envelope Approach to Modeling the Geometric Deviation of the Machined Surface for a Specific Five-Axis CNC Machine Tool*, International Journal of Machine Tools and Manufacture, 95, 67–77.
[16] FU G., GONG H., FU J., GAO H., DENG X., 2019, *Geometric Error Contribution Modeling and Sensitivity Evaluating for Each Axis of Five-Axis Machine Tools Based on POE Theory and Transforming Differential Changes Between Coordinate Frames*, International Journal of Machine Tools and Manufacture, 147, 103455.
[17] LI Q., WANG W., ZHANG J., SHEN R., LI H., JIANG Z., 2019, *Measurement Method for Volumetric Error of Five-Axis Machine Tool Considering Measurement Point Distribution and Adaptive Identification Process*, International Journal of Machine Tools and Manufacture, 147, 103465.
[18] BAMMERT K., STOBBE H., 1970, *Results of Experiments for Determining the Influence of Blade Profile Changes and Manufacturing Tolerances on the Efficiency, the Enthalpy Drop, and the Mass Flow of Multi-Stage Axial Turbines*, ASME Winter Annual Meeting, Turbo Expo, Power for Land, Sea, and Air, V001T01A003, doi:10.1115/70-WA/GT-4.
[19] BAMMERT K., SANDSTEDE H., 1976, *Influences of Manufacturing Tolerances and Surface Roughness of Blades on the Performance of Turbines*, Journal of Engineering for Power, 98, 29–36.
[20] CHEN L., LI B., JIANG Z., 2017, *Inspection of Assembly Error with Effect on Throat and Incidence for Turbine Blades*, Journal of Manufacturing Systems, 43, 366–374.
[21] GARZON V.E., DARMOFAL D.L., 2003, *Impact of Geometric Variability on Axial Compressor Performance*, Journal of Turbomachinery, 125, 692–703.
[22] DOW E.A., WANG Q., 2015, *The Implications of Tolerance Optimization on Compressor Blade Design*, Journal of Turbomachinery, 137, 101008.
[23] MONTOMOLI F., MASSINI M., SALVADORI S., 2011, *Geometrical Uncertainty in Turbomachinery: Tip Gap and Fillet Radius*, Computers & Fluids, 46, 362–368.
[24] LUO J., LIU F., 2018, *Statistical Evaluation of Performance Impact of Manufacturing Variability by an Adjoint Method*, Aerospace Science and Technology, 77, 471–484.
[25] WANG X., ZOU Z., 2019, *Uncertainty Analysis of Impact of Geometric Variations on Turbine Blade Performance*, Energy, 176, 67–80.
[26] XIA Z., LUO J., LIU F., 2019, *Performance Impact of Flow and Geometric Variations for a Turbine Blade Using an Adaptive NIPC Method*, Aerospace Science and Technology, 90, 127–139.
[27] ZHU Z.Q., ZHANG Y., CHEN Z.T., JIANG Z.P., 2020, *A Methodology for Measuring and Evaluating Geometric Errors of Aero-Engine Blades Based on Genetic Algorithm*. Proceedings of the Institution of Mechanical Engineers, Part B, Journal of Engineering Manufacture, 234, 260–269.
[28] SALEHI S., RAISEE M., CERVANTES M.J., NOURBAKHSH A., 2018, *On the flow field and performance of a centrifugal pump under operational and geometrical uncertainties*, Applied Mathematical Modelling, 61, 540–560.
[29] ZHANG W., ZOU Z., YE J., 2012, *Leading-Edge Redesign of a Turbomachinery Blade and its Effect on Aerodynamic Performance*, Applied Energy, 93, 655–667.
[30] WANG S., WEN F., ZHANG S., ZHANG S., ZHOU X., 2019, *Influences of Trailing Boundary Layer Velocity Profiles on Wake Vortex Formation in a High-Subsonic-Turbine Cascade*, Proceedings of the Institution of Mechanical Engineers, Part A: Journal of Power and Energy, 233, 186–198.
[31] SIEVERDING C., MANNA M., 2020, *A Review on Turbine Trailing Edge Flow*, International Journal of Turbomachinery, Propulsion and Power, 5/2, 10.
[32] DING H., LI Y., LAKZIAN E., WEN C., WANG C., 2019, *Entropy Generation and Exergy Destruction in Condensing Steam Flow Through Turbine Blade with Surface Roughness*, Energy Conversion and Management 196, 1089–1104.
[33] GAO J., GINDY N., CHEN X., 2006, *An Automated GD&T Inspection System Based on Non-Contact 3D Digitization*, International Journal of Production Research, 44, 117–134.

[34] BAUER F., SCHRAPP M., SZIJARTO J., 2019, *Accuracy Analysis of a Piece-to-Piece Reverse Engineering Workflow for a Turbine Foil Based on Multi-Modal Computed Tomography and Additive Manufacturing*, Precision Engineering, 60, 63–75.
[35] SHIMAZAKI H., SHINOMOTO S., 2007, *A Method for Selecting the Bin Size of a Time Histogram*, Neural Computation, 19, 1503–1527.
[36] STANISA B., IVUSIC V., 1995, *Erosion Behaviour and Mechanisms for Steam Turbine Rotor Blades*, Wear 186–187, 395–400.
[37] AHMAD M., CASEY M., SÜRKEN N., 2009, *Experimental Assessment of Droplet Impact Erosion Resistance of Steam Turbine Blade Materials*, Wear 267, 1605–1618.